AD-A139 122 ELECTRON ENERGY DEPOSITION IN THE MIDDLE ATMOSPHERE(U) 1/1
AEROSPACE CORP EL SEGUNDO CA SPACE SCIENCES LAB
A L VAMPOLA ET AL. 05 DEC 83 TR-0084(4940-05)-5
UNCLASSIFIED SD-TR-83-79 F04701-83-C-0084 F/G 4/1 NL

END
DATE FILMED
4-84
DTIC

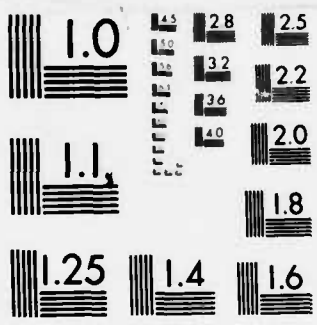

REPORT SD-TR-83-79

12

Electron Energy Deposition in the Middle Atmosphere

A. L. VAMPOLA and D. J. GORNEY
Space Sciences Laboratory
Laboratory Operations
The Aerospace Corporation
El Segundo, Calif. 90245

5 December 1983

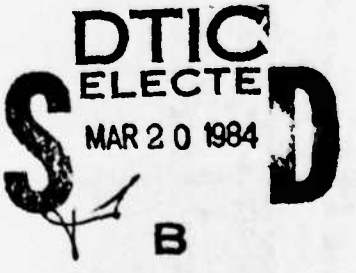

Prepared for
SPACE DIVISION
AIR FORCE SYSTEMS COMMAND
Los Angeles Air Force Station
P.O. Box 92960, Worldway Postal Center
Los Angeles, Calif. 90009

This report was submitted by The Aerospace Corporation, El Segundo, CA 90245, under Contract No. F04701-83-C-0084 with the Space Division, P.O. Box 92960, Worldway Postal Center, Los Angeles, CA 90009. It was reviewed and approved for The Aerospace Corporation by H. R. Rugge, Director, Space Sciences Laboratory. Captain Gary M. Rowe, SD/YCM, was the project officer for the Mission-Oriented Investigation and Experimentation (MOIE) program.

This report has been reviewed by the Public Affairs Office (PAS) and is releasable to the National Technical Information Service (NTIS). At NTIS, it will be available to the general public, including foreign nationals.

This technical report has been reviewed and is approved for publication. Publication of this report does not constitute Air Force approval of the report's findings or conclusions. It is published only for the exchange and stimulation of ideas.

Gary M. Rowe

Gary M. Rowe, Captain, USAF
Project Officer

Joseph Hess, GM-15, Director
West Coast Office, Air Force Space
Technology Center

UNCLASSIFIED

SECURITY CLASSIFICATION OF THIS PAGE (When Data Entered)

REPORT DOCUMENTATION PAGE		READ INSTRUCTIONS BEFORE COMPLETING FORM
1. REPORT NUMBER SD-TR-83-79	2. GOVT ACCESSION NO. A139128	3. RECIPIENT'S CATALOG NUMBER
4. TITLE (and Subtitle) Electron Energy Deposition in the Middle Atmosphere		5. TYPE OF REPORT & PERIOD COVERED
		6. PERFORMING ORG. REPORT NUMBER TR-0084(4940-05)-5
7. AUTHOR(s) A. L. Vampola and D. J. Gorney		8. CONTRACT OR GRANT NUMBER(s) F04701-83-C-0084
9. PERFORMING ORGANIZATION NAME AND ADDRESS The Aerospace Corporation El Segundo, California 90245		10. PROGRAM ELEMENT, PROJECT, TASK AREA & WORK UNIT NUMBERS
11. CONTROLLING OFFICE NAME AND ADDRESS Space Division Los Angeles Air Force Station Los Angeles, California 90009		12. REPORT DATE 5 December 1983 13. NUMBER OF PAGES 31
14. MONITORING AGENCY NAME & ADDRESS(if different from Controlling Office)		15. SECURITY CLASS. (of this report) Unclassified 15a. DECLASSIFICATION/DOWNGRADING SCHEDULE

16. DISTRIBUTION STATEMENT (of this Report)

Approved for public release; distribution unlimited.

17. DISTRIBUTION STATEMENT (of the abstract entered in Block 20, if different from Report)

18. SUPPLEMENTARY NOTES

19. KEY WORDS (Continue on reverse side if necessary and identify by block number)

Electron precipitation
D-region ionization
Atmospheric ionization

20. ABSTRACT (Continue on reverse side if necessary and identify by block number)

Spectra of locally precipitating 36 to 317 keV electrons obtained by instrumentation on the S3-2 satellite are used to calculate energy deposition profiles as a function of latitude, longitude, and altitude. In the 70 - 90 km altitude, midlatitude ionization due to these precipitating energetic electrons can be comparable to that due to direct solar H Lyman α. At night, the electrons produce ionization more than an order of magnitude greater than

DD FORM 1473 (FACSIMILE)

UNCLASSIFIED

SECURITY CLASSIFICATION OF THIS PAGE (When Data Entered)

19. KEY WORDS (Continued)

1/100 sq cm

20. ABSTRACT (Continued)

that expected from scattered H Lyman α. Maximum precipitation rates in the region of the South Atlantic Anomaly are on the order of 10^{-2} erg/cm^2-sec with a spectrum of the form $j(E) = 1.34 \times 10^5 E^{-2.27}$ (keV). Southern hemisphere precipitation dominates that in the north for $1.1 < L < 6$ except for regions of low local surface field in the northern hemisphere. Above $L = 6$, local time effects dominate; i.e., longitudinal effects due to the asymmetric magnetic field which are strong features below $L = 6$ disappear and are replaced by high-latitude precipitation events which are local-time features.

134000 X 1/E to the 2.27 power

PREFACE

The data processing, reduction, and analysis portions of this study were supported, in part, by National Science Foundation Grant ATM-77-28187.

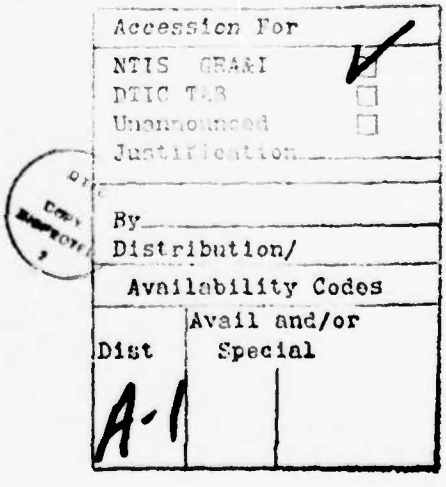

CONTENTS

FIGURES

I. INTRODUCTION

The study of atmospheric ionization sources has been a topic of considerable interest for a number of years (see, for example, Rosenberg and Lanzerotti (1979) and references therein). Middle-atmospheric ionization due to energetic particle or electromagnetic wave penetration affects the propagation of VLF communications signals (Potemra and Zmuda (1970)), and Crutzen et al. (1975), Thorne (1977) and Reagan et al. (1978) have suggested that minor neutral species concentrations might be significantly affected by variations in the middle atmospheric energy input. Other effects of magnetospheric and extraterrestrial penetrating radiation, including possible influences on weather-related phenomena (e.g., Roberts and Olson (1973a, b); Markson (1978)) and atmospheric aerosol formation (Mohnen and Kiang (1978)) have been discussed.

Galactic cosmic rays, solar X-rays and H-Lyman α emissions, energetic solar protons, auroral electrons, and energetic precipitating radiation belt electrons and their associated bremsstrahlung X-rays have been identified as significant middle-atmosphere ionization sources (see reviews by Potemra and Zmuda (1970); Potemra (1973, 1974); and Reagan (1977)). For each of these ionization sources, attempts have been made to estimate the long-term "average" ionization rates as a function of altitude and latitude, as well as the variations expected during strong "events." In this report we concentrate on evaluating the long-term contribution of precipitating magnetospheric electrons to middle atmosphere ionization in the high, middle and low latitude regions. The extremely large data set acquired by the S3-2 spacecraft (over 10^7 samples per channel) has allowed us to examine the latitude and geographic longitude dependence of electron precipitation. For example, we can compare precipitating electron fluxes and their atmospheric effects in regions of anomalously low surface magnetic field (such as the South Atlantic Anomaly (SAA)) to longitudinally averaged values (see Gledhill (1976), Torr et al. (1976), and Gledhill and Hoffman (1981) for examples of previous attempts at observing SAA precipitation features). The present study comprises the first

documentation of long-term average electron precipitation over the range 1.1 < L < 6.0, with global geographic coverage including resolution of regions such as the SAA.

Gough and Collin (1973), Larsen et al. (1976) and Spjeldvik and Thorne (1975, 1976) have discussed the possible importance of midlatitude electron precipitation to middle atmosphere ionization. We extend these observations to the very low latitude regions and show that while the long-term ionization effects of radiation belt electron precipitation are dominated by that due to solar H Lyman α during the daytime, electron precipitation can dominate the ionization due to scattered H Lyman α radiation at night in the altitude region near 80 kilometers, and particularly in regions of anomalously low surface magnetic field.

Direct measurements of the precipitating electron fluxes are extremely difficult. As a result, estimates are usually made on the basis of indirect analyses. Several alternate methods are: measurement of forward-scattered X-ray flux using rocket-borne instrumentation at altitudes below the range of directly-penetrating particles; measurement of the fluxes in the drift loss-cone and calculation of average loss-rates from the geometry of the atmosphere and the drift shell as a function of longitude and local time; measurement of life-times of particles in the inner zone (as was done with the Starfish electrons) and determining average precipitation rates. The problems with these last two methods primarily involve the assumption that the interaction with the atmosphere occurs only in the anomaly region and the fact that the methods rely heavily on assumptions about the rate of pitch-angle diffusion in the drift loss cone. The first method is limited by the fact that rocket measurements are made for only a brief interval of time, resulting in low statistics and temporally isolated data. Average conditions may be far different from the instantaneous conditions which exist during any single rocket flight.

Satellite measurements of the precipitating electron flux should be much more useful, since a satellite can make repeated measurements over widely varying magnetic conditions, longitudes, local times, etc. The drawback to

such a method is basically a problem of background in the sensor. Particles precipitating in the region of the South Atlantic Anomaly may have pitch-angles very close to those of stably-trapped particles (since those particles which just miss interacting with the atmosphere at the longitude of the SAA will continue to drift in longitude until something perturbs their pitch-angles to lower their mirror altitudes). For practical purposes, the atmosphere at 100 km can be considered the boundary between zero absorption and total absorption, although absorption is an exponential process for which the effects in energetic electrons can be readily seen over the range of about 95 km to 105 km. The stably-trapped particle population in the L region of interest here also includes very energetic protons, E > 50 MeV, which completely penetrate the spacecraft, its instrumentation, and any detectors attempting to make measurements of the precipitating electron flux.

In the heart of the inner zone, a 1 cm^2 detector would be penetrated by more than 2000 protons per second. Larger detectors would experience a proportionately larger background. That same detector, with a nominal solid angle defined by its viewing aperture, might see an equivalent number of electrons with an energy within its passband. These electrons would be almost entirely stably-trapped. The proportion of electrons which would be in the local bounce loss cone would be down by several orders of magnitude, unless there were a strong diffusion process acting upon them (such as occurs in the auroral regions and occasionally in the inner zone in conjunction with whistlers or transmitting stations). Hence, in order to make measurements of the precipitating flux, particularly in the region of the SAA, care must be taken to discriminate against the penetrating background.

II. INSTRUMENTATION

The electron data were acquired by a 180° magnetic electron spectrometer similar to those described previously (Vampola, (1969)) except that the analyzing field was 380 gauss and the aperture acceptance angle was ± 7°. Eight differential energy channels had energy centroids at 36, 62, 117, 132, 176, 217, 267, and 317 keV. The spectrometer was carried on the S3-2 satellite which had apogee and perigee altitudes of 1570 and 248 km at launch, an inclination of 96.3 degrees, and was spin-stabilized at 3 rpm, with the spin-vector normal to the orbit plane. The spectrometer aperture viewed normal to the spin vector, enabling pitch-angle sampling well within the bounce loss cone virtually all of the time. The data used in this study were acquired during a 20-month period between December 1975 and August 1977. An on-board magnetometer was used for determination of local pitch-angle for particle studies.

Since background subtraction is an essential step in this analysis, a detailed discussion of the spectrometer and its on-board data processing is warranted. Electrons incident through a disc-loaded collimator are focussed through 180° upon an array of silicon detectors. Nominal depletion depth of the rectangular (1 cm × 1.5 cm × 1 mm) dies was 1000 microns. This corresponds to an energy deposit of about 400 keV for a minimum ionizing particle which penetrates 90° to the rectangular area. The highest energy channel had a nominal upper limit of 340 keV for electrons focussed upon its detector. Each electron channel detector had a set of pulse analyzing electronics which was set with a lower threshold of 50% of the nominal lower energy limit of momentum focussing for that channel and an upper threshold of 110% of the nominal highest energy limit. Energy deposits exceeding this upper threshold were considered to be due to penetrating protons and were rejected. A ninth detector was shielded from focussed electrons and was used to monitor bremsstrahlung and penetrating protons (upper threshold set at 350 keV). Protons which did not penetrate through the entire thickness of the silicon die produced lower energy deposits. These "corner cutters" mimic true electron signals. Geometric considerations indicate that about 5% of the solid angle

subtended by the silicon die provides path-lengths shorter than the minimum required for proton rejection. Hence, there is a residual background due to penetrating protons which is not eliminated by the on-board processing. Techniques for identifying this residual background and eliminating it during post-processing were required in order to accomplish the present study. If the instrument were in a proton background which produced 10^3 counts per second in the proton monitor, a count rate of about 50 per second uncorrected background could be expected in a typical channel. If the precipitating electrons produced only a few counts per second in the detector, they would be unobservable unless very good statistics were available and the correction for this residual background were known very accurately.

III. PROTON CORRECTION

Approximately 6×10^5 data samples (counts integrated for one second per sample) were averaged in which the following criteria were met: proton monitor count > 100; instrument aperture view angle, when corrected for both finite acceptance angle and angular scan, completely within the downward viewing local atmospheric loss cone; count in a typical electron channel < 12% of the proton monitor count. The second condition was imposed to ensure that virtually no real electron counts would be present in the data sample, since the reflection coefficient for electrons in our energy range mirroring below 100 km is less than 1% (determined by examining polar region pitch-angle distributions during solar flare electron events). For measurements in the eV to a few keV range, secondaries and backscattered primaries can be a more significant factor (Stamnes (1981)). The third condition was imposed to reject samples in which there might be local strong precipitation processes operating (as near high-powered VLF stations and their conjugate points). The resultant summations of counts in each of the electron channels were normalized to the integrated proton monitor count (about 2×10^8 total counts). Ratios were in the range of .04 to .06 for all channels but one. That one had had a failure of the rejection circuitry and the ratio was 1.0678 (which is consistent, since it counted not only the regular protons being counted by the proton monitor, but also the "corner cutters" which left energy deposits within the electron acceptance band).

The limitation on the validity of the proton corrections is set not only by the statistical accuracy of the determination, but also by uniformity in responses of both the proton monitor and the electron channels to "corner-cutting" proton background with variations in the proton energy spectrum. Since the specific ionization of a proton traversing a silicon detector increases with decreasing energy, the geometric factor for "corner-cutting" background protons also decreases with decreasing energy of the incident proton. For the conditions of this experiment, the proton monitor response is essentially independent of the proton energy spectrum. However, the minimum

energy required for a proton to penetrate the instrument and reach an electron detector is 70 MeV, with the average energy being over 100 MeV. In the inner zone, the proton spectrum is very hard and does not change radically above 70 MeV as a function of L. But the spectrum is softer at higher L in the inner zone, and a small effect was visible in the analysis. Hence the correction is insufficient at the region where the proton spectrum is hardest and is excessive at the outer edge of the inner zone where the spectrum is softest (due to the fact that data from the entire inner zone were averaged in the background analysis). The error due to variations in the proton energy spectrum is of the same order as the error due to statistics (approximately 0.5% to 1% of the background correction for the various channels for the data set used for the electron energy deposition measurements).

IV. ELECTRON DATA PROCESSING

Preliminary analyses using a small portion of the total data set indicated that the average electron precipitation rate in the South Atlantic Anomaly was quite small, corresponding to several counts per second or less in an individual detector. Since these "true" counts would also be accompanied by uncorrected, though partially correctable, background counts, it was decided that the error due to these background counts should be minimized by selecting portions of the orbit in which the proton background was very low; i.e., the satellite itself should be low on the field line rather than in the heart of the inner zone. Selecting only data obtained at low altitude should have negligible effect on the electron counting rate since the measured electrons would be in the local loss cone and previous measurements had shown that the loss-cone distribution is essentially isotropic. Liouville's theorem (conservation of density in phase space) predicts that the count rate in the loss cone will be independent of altitude. There is a strong dependence of proton flux with altitude (because of the long residence time of the energetic protons and interactions with the residual atmosphere). Thus, by selecting low altitude data, we can reduce the background contribution while maintaining the signal count rate. The limit on reduction of the background by this method is set by a requirement for a sufficient number of samples in the data set to have sufficiently good statistics for a valid background subtraction. By reducing the altitude, we reduce the total number of data samples in our set.

Data samples were included in the electron analysis only if two conditions were met: 1) the total count in the proton monitor was less than 20 (resulting in a background count of less than one in the electron channels); and 2) the instrument aperture direction, when corrected for finite acceptance angle and angular scan during the sample period, included only pitch-angles corresponding to a mirror location at or below 100 km on this half-bounce period (i.e., the instrument was looking up the field line at locally precipitating particles). Figure 1 presents the average precipitation electron

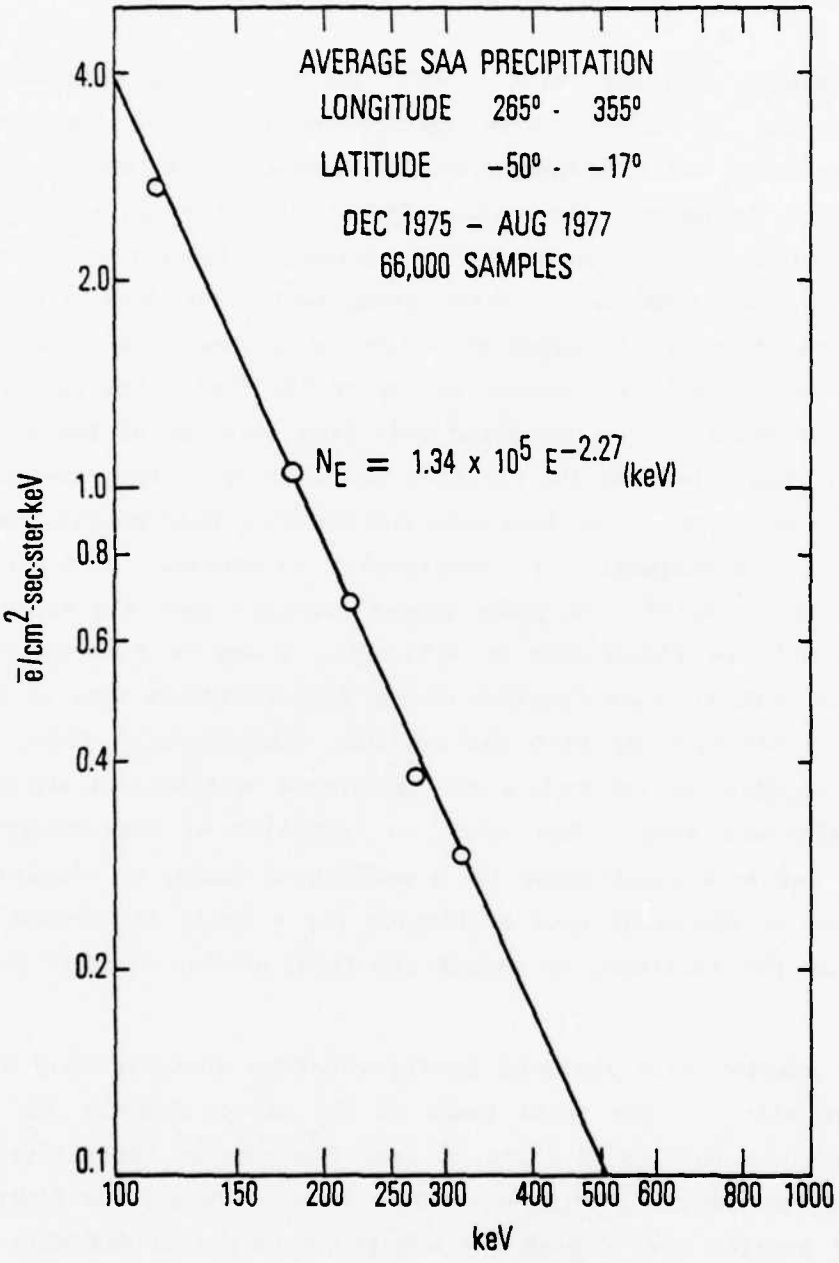

Figure 1. Energy spectrum of the average quiet-time electron precipitation in the region of the South Atlantic Anomaly.

spectrum for the South Atlantic Anomaly. For these data, a requirement was placed that the 100-km point on the field line in the local hemisphere be between 265° and 355° east longitude and between -50° and -17° latitude. The background correction had sufficient statistical accuracy to provide a residual error of less than 1%. The spectrum probably becomes flatter at lower energies. The lowest energy channel, 36 keV, measured an average flux of 23 e^-/cm^2-sec-ster-keV. However, this channel and two others (62 and 132 keV) occasionally responded to noise produced by voltage breakdown in another instrument on the satellite. The correction for this on-board "coherent" noise is good to about 10%. The correction was made by plotting the channels and visually estimating the average interfering count rate. When this "coherent" noise source is present, it is frequently in the hundreds of counts per second range in the first two channels (tens of counts per second in the 132-keV channel). Since the instantaneous corrections are significant compared to average true fluxes in these channels, we feel that the confidence that can be placed in those channels in this analysis (where an exceptionally accurate background correction must be made) does not warrant including them in Figure 1. The "measured value" for the 36 keV electrons is lower than an extrapolation of the spectrum of Figure 1 (23 vs 39.6 for the extrapolation). We feel that this difference can be taken as an indication that the spectrum probably flattens out at lower energies but the confidence level of the result does not warrant a quantitative conclusion. AE-C data obtained in the anomaly region in 1976 show that the energy spectrum of 0.2 to 27 keV electrons is harder than the one we measure for an average flux at higher energies (Gledhill and Hoffman (1981)). Their discrete spectra fit power-law curves with exponents in the range -0.96 to -1.18. In their energy range, there is probably a significant component of secondary and backscatter electrons from the opposite hemisphere. The individual spectra merge with our average spectrum surprisingly well. For all of the data presented here, with the exception of the 36 keV channel plots of Figure 2, which are presented for comparison purposes, the known error limits due to background corrections and the statistical uncertainty in those corrections is less than 5%. In general, the other channels are consistent with the results presented here.

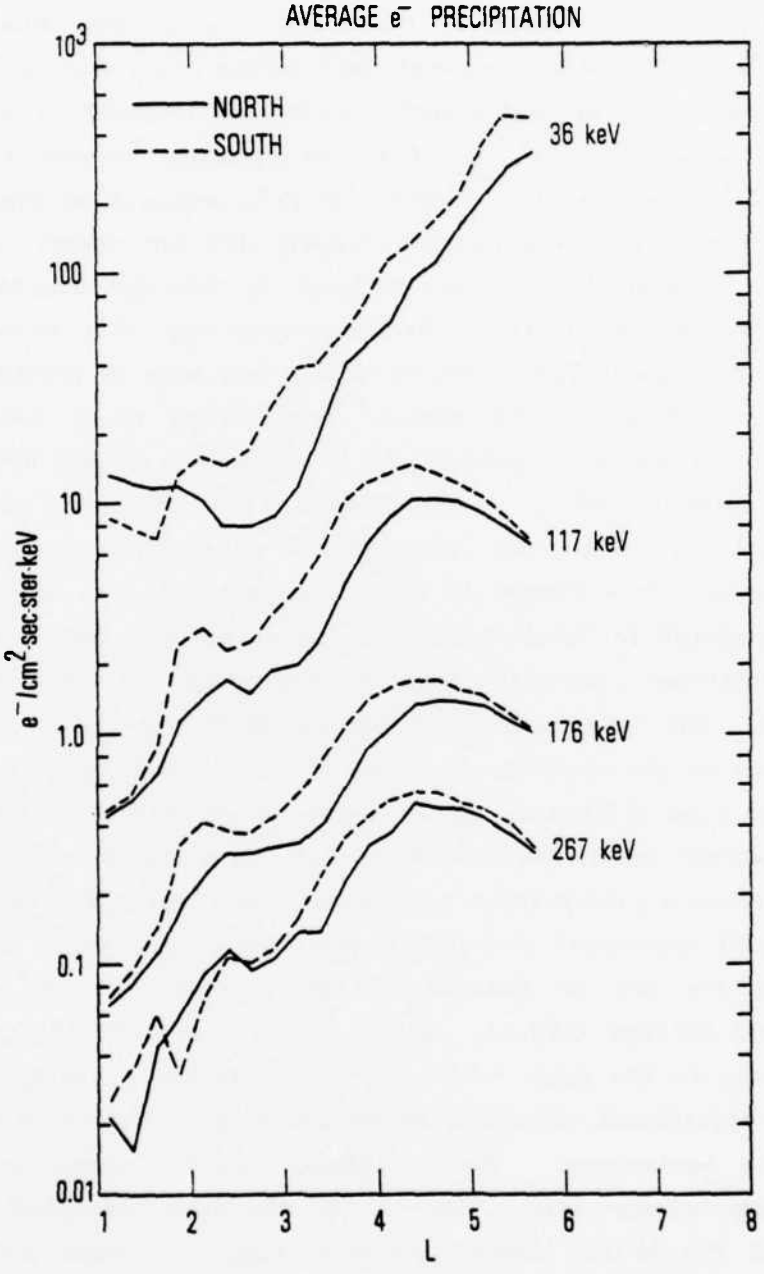

Figure 2. Average quiet-time electron precipitation as a function of L. Data are averaged over all longitudes. The relative peak near L=2 is probably due to enhanced precipitation caused by ground-based VLF transmitters (Vampola, 1977).

V. RESULTS

The spectrum presented in Figure 1 can be integrated to determine the total average precipitated energy flux. The total energy flux above 45 keV is 1.01×10^{-3} ergs/cm^2-sec. If, instead of extrapolating the spectrum of Figure 1 down to 45 keV, one makes the extreme assumption that the spectrum is completely flat between 45 keV and 100 keV, the integrated energy flux is 8.2×10^{-4} ergs/cm^2-sec, only a reduction of 19% from the other estimate. Thus, the energy integral is not very sensitive to the shape of the spectrum below 100 keV. Both of these integrations assume that there is no significant flux above 1 MeV (based on higher altitude measurements of the trapped flux).

Figure 2 presents plots of average precipitated flux as a function of L. For these plots, the precipitated flux was averaged over all longitudes, even though most of the flux was actually observed precipitating in the region of the South Atlantic Anomaly (Figure 3). The plots show that precipitation is consistently greater in the southern hemisphere than in the northern. The increase in precipitation at very low L in the northern hemisphere in the 36 keV channel is probably partially due to degraded higher energy electrons and secondary electrons emerging from the SAA. The enhancement around L=2 in all channels is probably due to VLF transmitter effects (Vampola and Kuck (1978); Koons et al. (1981); Imhof et al. (1981)), even though the data selection process would have edited out any data samples in which strong local precipitation was occurring.

Figure 3 is a pseudo-3D plot of the average precipitation energy flux as a function of longitude and latitude in the SAA. Lines of constant L and constant B at 100 km are included. The peak energy flux is about 2×10^{-2} erg/cm^2-sec. Data were summed in $3° \times 3°$ longitude-latitude bins for this plot. The energy integral was obtained by assigning the measured electron flux in each acceptable channel to an energy width which was symmetrical around the nominal channel energy and extended half way to the next energy channel; that is, a histogram energy spectrum was generated from the measured data and summed. Fluxes below 67 keV and above 340 keV were arbitrarily

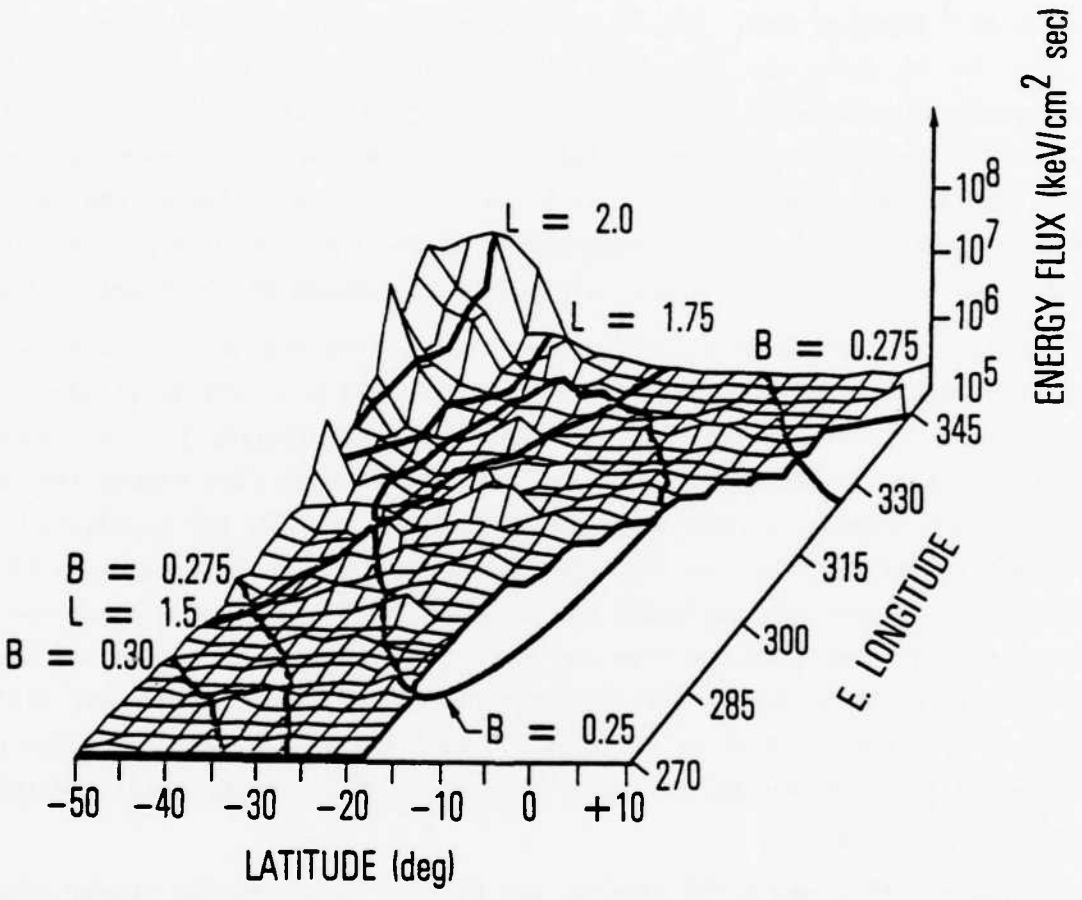

Figure 3. Pseudo 3-D plot of the energy flux of electrons precipitated in the region of the South Atlantic Anomaly. Only quiet-time data are included.

assigned a value of zero. The error in energy flux due to zeroing out fluxes above 340 keV is less than 10%.

Figures 4 and 5 are plots of energy deposition as a function of East Longitude for L values of 2.0 - 2.25 and 4.0 - 4.25, respectively. Separate curves are presented for the northern and southern hemispheres on each plot. Also, the magnitude of the magnetic field at 100 km altitude, B_{100}, is plotted as a function of longitude for comparison purposes. The energy flux maximizes in the same hemisphere as the minimum B_{100} for both L intervals. However, there is only about a factor of 3 difference in energy deposition rate between the north and south latitudes at longitudes where the difference in B_{100} is large. The ratio of northern to southern energy deposition can be taken as an indication that perhaps as much as 50% of the electrons pitch-angle scattered in the northern hemisphere mirror above the atmosphere and then are lost in the other hemisphere. If pitch-angle scattering were a slow diffusion process (e.g., Lyons et al. (1972), Lyons and Thorne (1973)), we would expect virtually all of the energy deposition to occur in the hemisphere with the lower B field at 100 km. The atmosphere in the hemisphere with the higher B_{100} would receive only backscattered electrons from the lower B_{100} hemisphere (at most a few percent for these energies). This is clearly not the case. Hence, we can state that electron pitch-angle scattering involves scattering in discrete events rather than a diffusive process.

Figures 6 and 7 present plots of precipitating electron flux as a function of local time for various energy channels for the intervals $6 < L < 9$ and $9 < L < 13$. At these latitudes, local time rather than longitude is the controlling factor. In contrast to the data of Figures 1 - 5, these precipitation data include intense events. Correction for bremsstrahlung background was accomplished by subtracting counts obtained while the aperture was oriented in the downward looking loss cone from the counts obtained while the aperture was oriented in the upward looking loss cone. Since there is a small backscattered flux component in the upcoming direction, these data represent a net precipitation flux (absorbed by the atmosphere) rather than the total downgoing flux. The difference between north and south fluxes was smaller than the statistical and temporal variations between different data

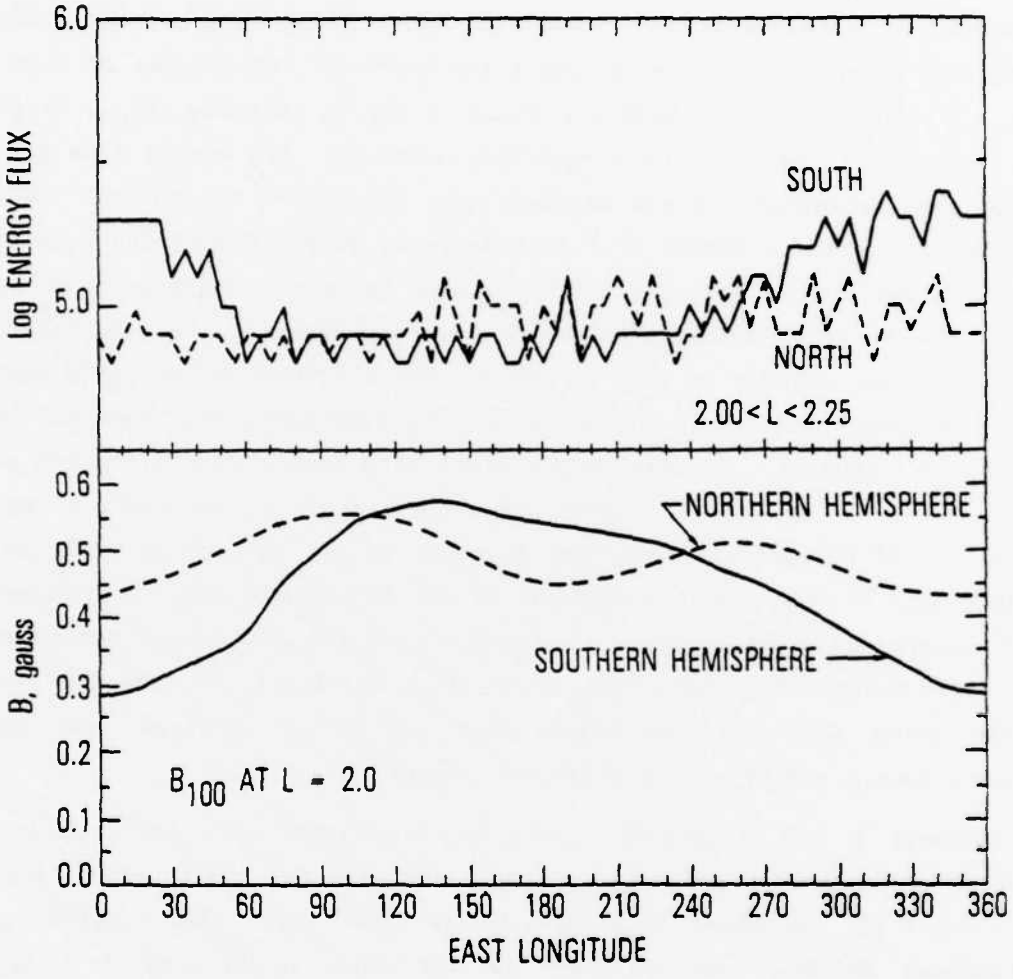

Figure 4. Plot of precipitating electron energy flux (keV cm^{-2} sec^{-1}) as a function of longitude for both the northern and southern hemispheres in the interval $2.0 < L < 2.25$. The magnetic field intensity at 100 km, B_{100}, is also plotted for comparison. The tendency is for more flux to be precipitated in the hemisphere with the weaker field. If pitch-angle diffusion of the electrons were a slow process ($\Delta\alpha_{eq} \approx 1°/\tau_{1/2\ B}$, where α_{eq} is the equatorial pitch angle and $\tau_{1/2\ B}$ is the half-bounce period), essentially all of the energy deposition would occur in the hemisphere with the lower field intensity.

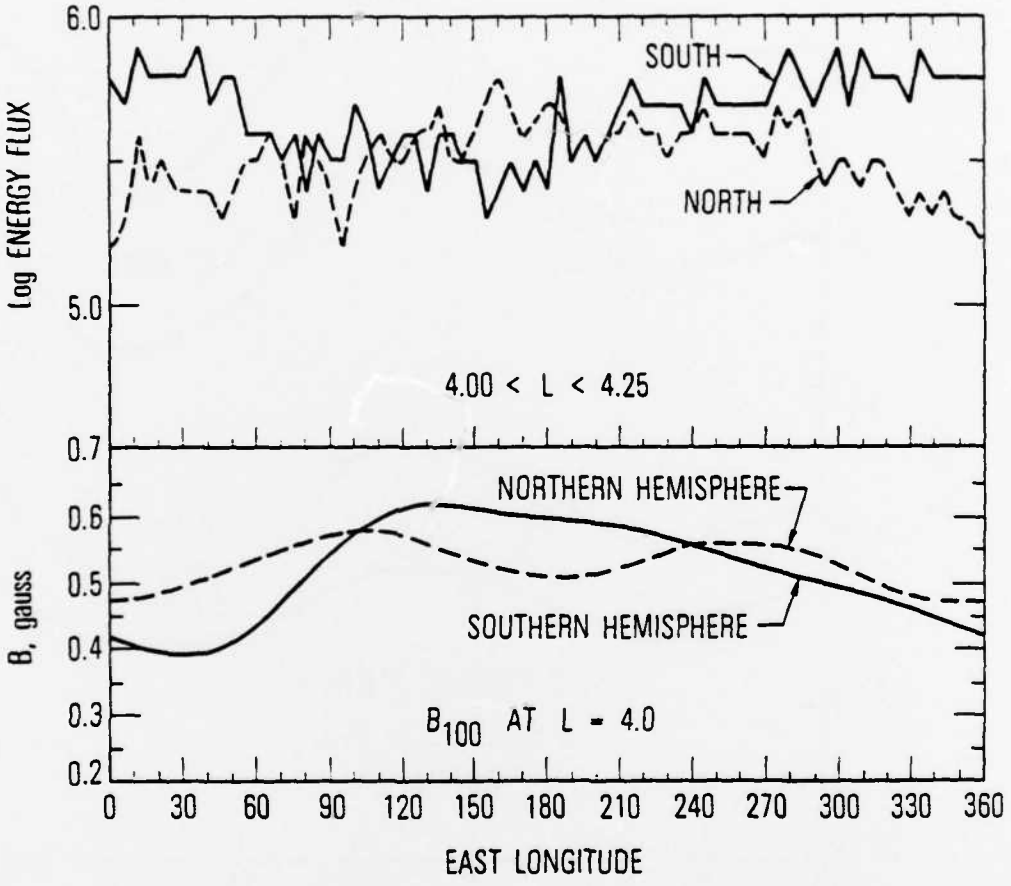

Figure 5. Plot similar to Figure 4, but for the interval 4.0 < L < 4.25.

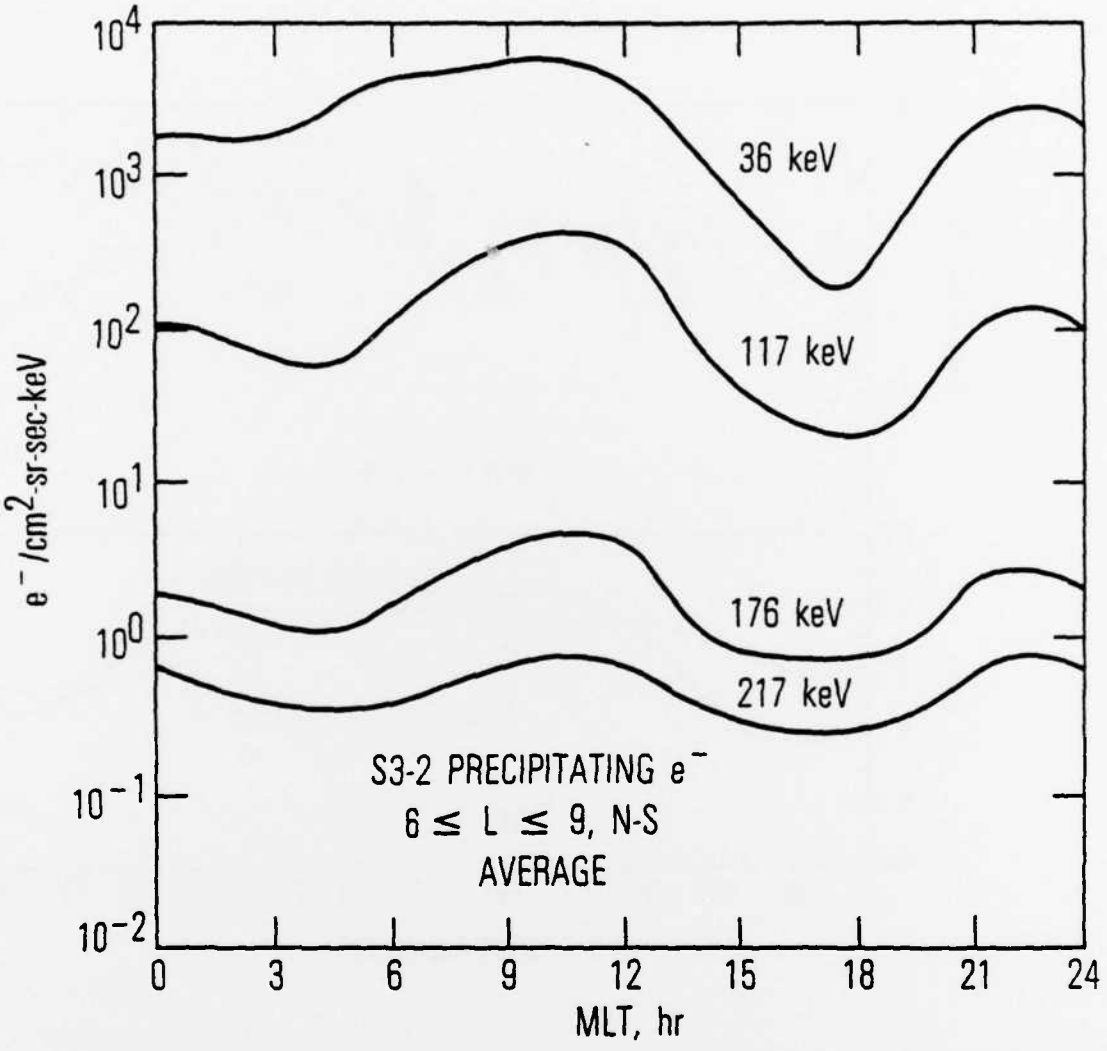

Figure 6. Plot of the average intensity of precipitated electron fluxes in several energy intervals as a function of local time. Data were averaged for all longitudes and latitudes corresponding to the region $6 < L < 9$. Data include strong precipitation events.

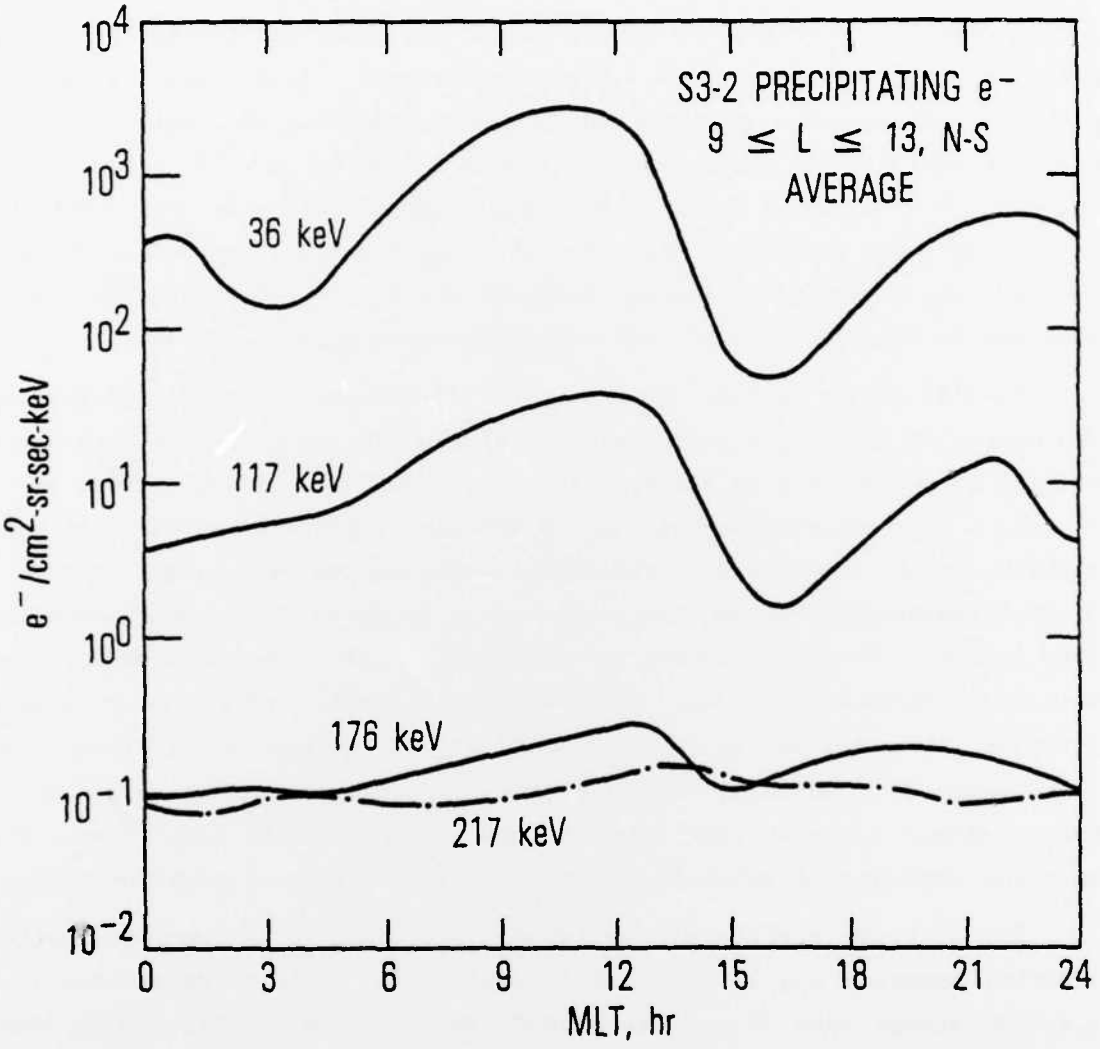

Figure 7. Plot similar to Figure 6, but for the region $9 < L < 13$. This region is beyond the outer zone limit for more energetic electrons most of the time.

sets in the same hemisphere, so both north and south fluxes were averaged together. Note that although these are average fluxes, a typical data sample had either virtually no flux or a fairly high flux, since the outer edge of the outer zone tends to be a region of intense precipitation with virtually no flux outside this region and only weak precipitation inside it. The variability in location of this outer edge produces the large scatter in the amount of precipitating flux observed in a given data sample. Still, significant local-time and L dependences are apparent in the statistical data set. The average precipitating flux at all energies is lower in the $9 < L < 13$ interval than in the $6 < L < 9$ interval because the outer edge of the outer zone tends to be within the lower interval. Note that the higher energy electrons, 176 keV and 217 keV, are almost at background level in the $9 < L < 13$ interval. Electrons observed in this interval are predominantly low energy electrons.

To this point we have described the latitudinal, zonal, and geographic dependence of the long-term average energy flux due to radiation belt electron precipitation, as well as the spectral variation over $1.1 < L < 6.0$. In order to make a reasonable assessment of the relative importance of electron precipitation as an atmospheric ionization mechanism we must also look at the altitude dependence of the ionization rates expected from the observed electron spectra. These ionization rate profiles in altitude can then be compared with other estimates of long term average ionization rates due to competing processes at equivalent altitudes and latitudes. Here we specifically compare our estimates of precipitating energetic electron ionization rates to those due to direct and scattered solar H Lyman α and galactic cosmic rays, and to previous estimates of midlatitude precipitating electron ionization rates.

The altitude profile of ionization rates due to a given precipitating electron spectrum can be calculated knowing the altitude dependence of the electron energy loss (e.g., Rees, 1963; Berger et al., 1970, 1974; Walt et al., 1969; Banks et al., 1974; Luhmann, 1976). The ionization rate is computed from the electron energy loss profile by assuming that one electron-ion pair is produced for each 35 eV of incident electron energy loss. We have used the approximate analytic technique described by Luhmann (1976) to determine the ionization rate profiles due to a primary incident electron spectrum, and have also calculated the low-altitude ionization rates due to downward-propagating bremsstrahlung X-rays (Luhmann (1977)).

Figure 8 shows ionization rate profiles for incident spectra representing zonal averages of the electron precipitation at L = 2, 4 and 5.75, along with an average over the South Atlantic Anomaly region defined earlier in this report. The peaks near 75 - 90 km altitude are due to primary electron energy deposition, whereas the secondary peaks near 35 - 45 km are due to bremsstrahlung X-ray penetration. As expected from the spectral variations shown in Figure 2, the magnitude and peak altitudes of ionization are rather L-dependent. Generally, the magnitude of the ionization rate increases with increasing L due to the stronger precipitation at higher latitudes, while the altitude of the peak ionization increases with increasing L, due to a softening of the precipitating spectrum toward higher latitudes. The SAA average spectrum is somewhat harder than the L=2 average, so SAA precipitation penetrates deeper into the atmosphere and can lead to more enhanced ionization from bremsstrahlung at low altitudes.

Two of these ionization rate profiles are reproduced in Figure 9, where they are compared with estimates of the ionization due to direct and scattered solar H Lyman α and galactic cosmic rays. The cosmic ray ionization is shown for a variety of latitudes, and for solar maximum and minimum periods. The solar H Lyman α ionization estimates are from midlatitude rocket measurements of the resonance fluorescence of nitric oxide (Meira (1971)). Interpretations of these data by Meira (1971) and Strobel (1972) are both plotted in Figure 9 (partially reproduced from Rosenberg and Lanzerotti (1979)).

While cosmic ray ionization certainly dominates long-term midlatitude electron precipitation below about 65 km altitude, electron precipitation can be an important ionization source in the 70 - 80 km range, where it even competes with the direct H Lyman α estimates. It appears that electron precipitation dominates the effects of scattered H Lyman α at all latitudes, and can therefore be of principal importance in maintaining the nighttime D-region of the ionosphere. It should be noted in comparing these quantities that the precipitating electron results presented here represent average "background" values, and that "events" can instantaneously produce much larger precipitating fluxes (e.g., Andreoli, 1980).

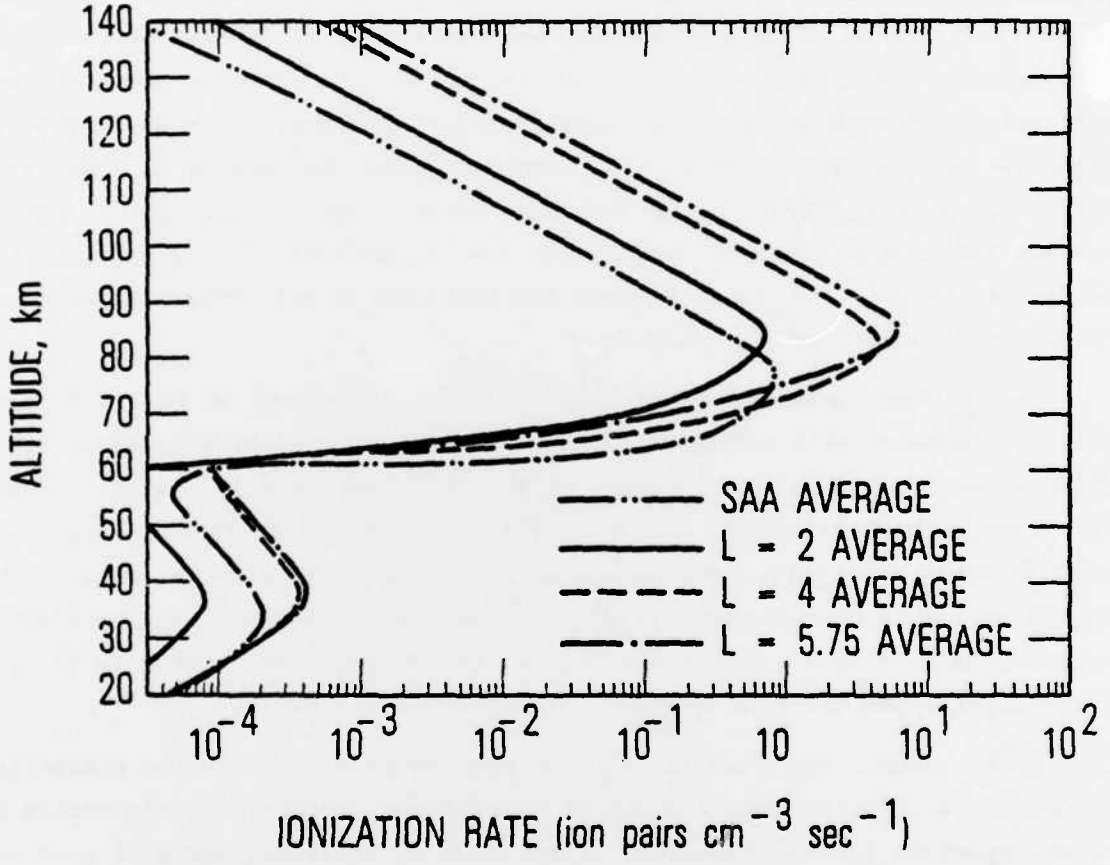

Figure 8. Plots of ionization rates as a function of altitude for the average electron precipitation spectra shown in Figs. 1 and 2. The peak around 80 km is due to the primary electrons, whereas the secondary peak around 40 km is due to bremsstrahlung X-rays.

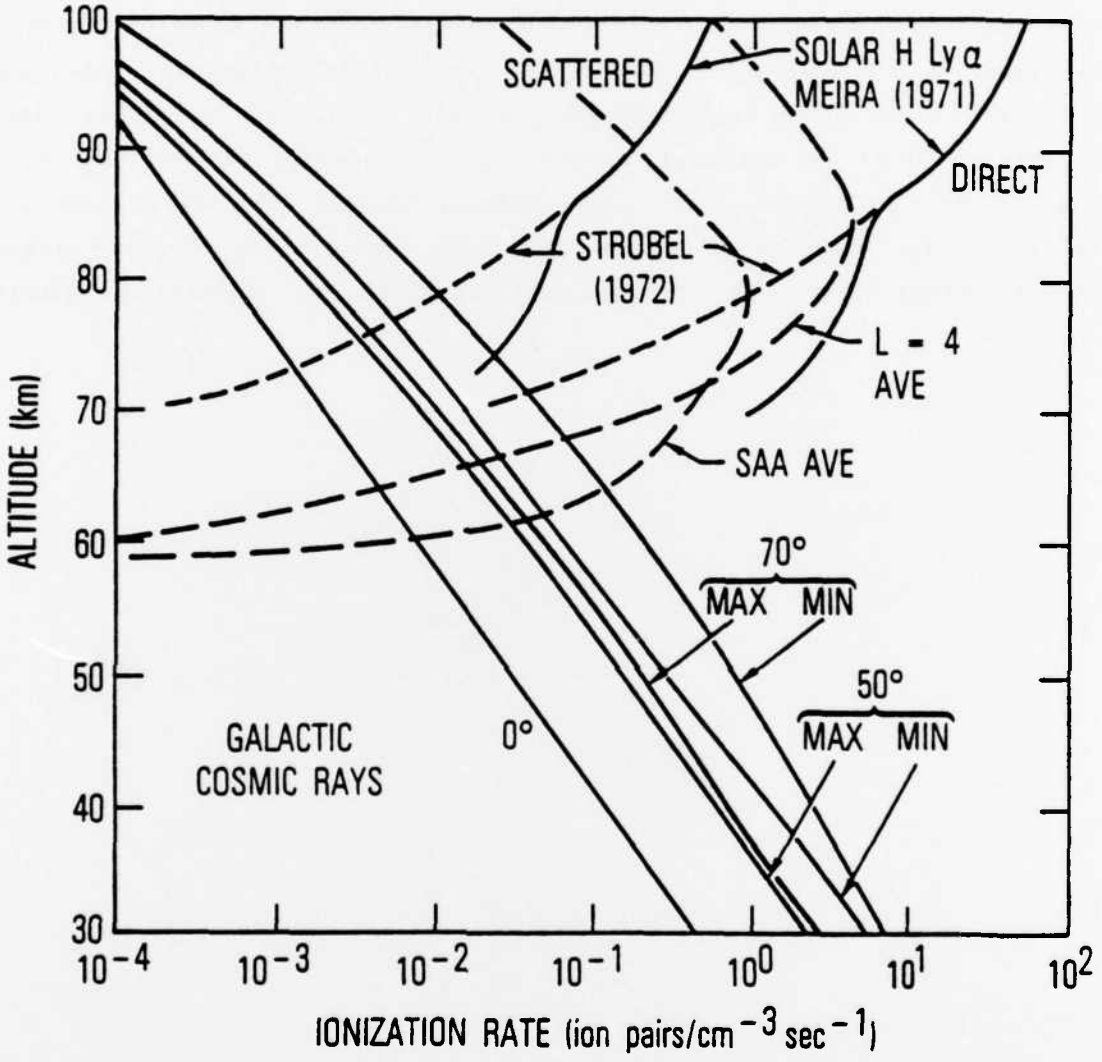

Figure 9. Comparisons of the ionization rate as a function of altitude for the electron energy spectrum of Figure 1 and the energy spectrum at L=4 from Figure 2 with ionization rates due to solar H Lyman α and galactic cosmic rays. For altitudes near 65 km, the direct electron precipitation ionization rate can exceed those of the other sources.

In Figure 10, we compare our zonal average midlatitude (L=4) results with previously published results from both rocket and satellite data. Potemra and Zmuda (1970) produced three models for precipitating electron spectra representing the range of intensities and hardness of available satellite and rocket data in midlatitudes. Their model A fits the upper range of the available data while models B and C represent less active conditions. Also shown in Figure 10 are other rocket (Tulinov et al. (1969)) and satellite (Manson and Merry (1970)) estimates of ionization, presented by Potemra (1973). As expected, the midlatitude (L=4) zonal average results from the present study fall within the brackets of Potemra and Zmuda's extreme models, and probably give a better long-term average representation of midlatitude electron ionization.

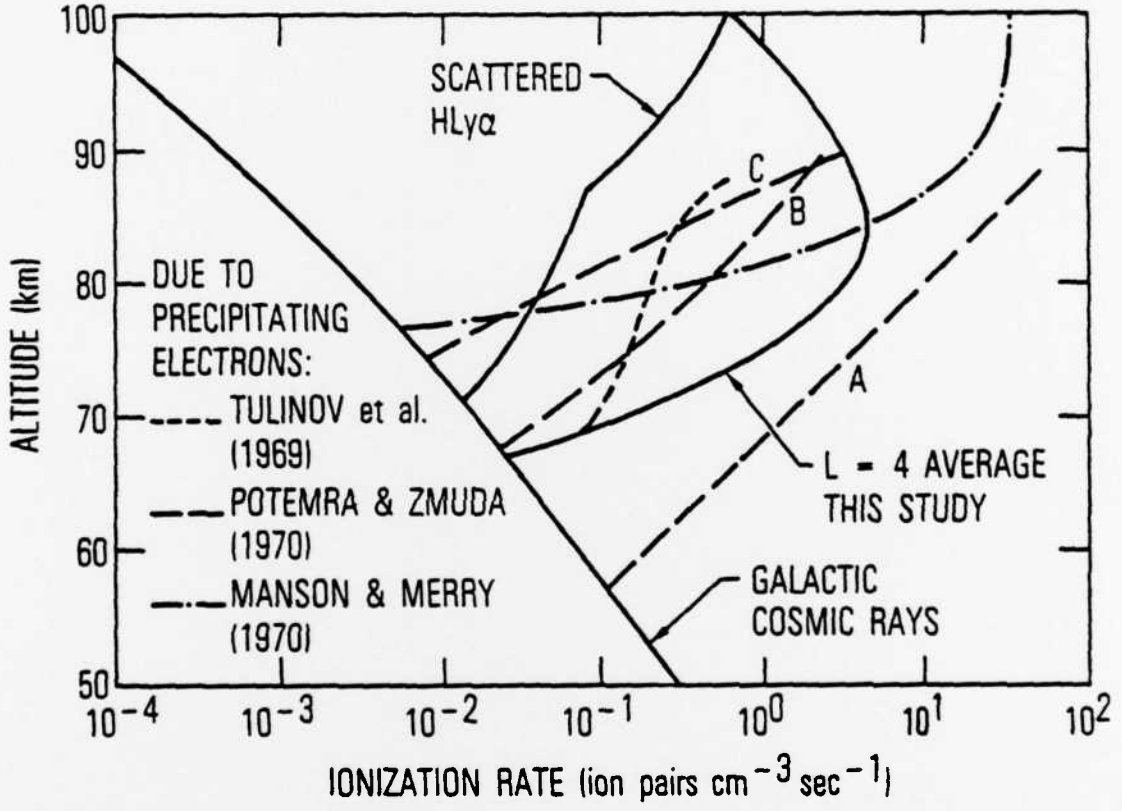

Figure 10. Comparison of the ionization rate as a function of altitude of the average L=4 spectrum from this work with measurement and estimates of the ionization rate from other satellite and rocket data.

VI. SUMMARY

We have analyzed a very large set of energetic electron data at mid- and low latitudes from the low altitude polar orbiting S3-2 spacecraft. The size of the data set has allowed good statistical sampling in latitude and longitude, and good coverage of local features such as the South Atlantic Anomaly. A great deal of effort was expended to accurately discriminate precipitating electron observations from the penetrating background signal.

The data were organized in longitude-latitude bins, and longitude-L bins, with northern and southern hemisphere data separated. Precipitation enhancements in the region of the South Atlantic Anomaly were observed, with the maximum precipitation occurring along the trough of anomalously low surface magnetic field extending south and east of the SAA. Maximum precipitation rates in the region of the SAA are on the order of 10^{-2} erg/cm^2 sec with a characteristic spectrum of the form $j(E) = 1.34 \times 10^5 E^{-2.27}$ (keV) e$^-$/cm^2 sec ster keV. Southern hemisphere precipitation dominates that in the north throughout the latitude range $1.1 < L < 6.0$ except in local regions of low surface field in the northern hemisphere. The precipitating spectrum softens considerably toward higher latitudes ($L > 4$).

Altitude profiles of the atmospheric ionization expected from the observed precipitating spectra were computed and compared to other sources of ionization. Ionization from midlatitude electron precipitation maximized in the altitude range 70 - 90 km, and can be comparable in those altitudes to the ionization due to direct solar H Lyman α. At night, electron precipitation ionization is more than an order of magnitude larger than that expected from scattered H Lyman α. Galactic cosmic ray ionization dominates at altitudes below about 65 km at all latitudes.

Results of this analysis were shown to be consistent with previous observations of midlatitude electron precipitation where comparisons were applicable. This report presents a "long-term" representation of midlatitude electron precipitation, with a strong statistical base and good geographic coverage.

REFERENCES

Andreoli, L. J., Relativistic electron precipitation: An observational study, Ph. D. Dissertation, University of California, Los Angeles, 1980.

Banks, P. M., C. R. Chappell and A. F. Nagy, A new model for the interaction of auroral electrons with the atmosphere: spectral degradation, backscatter, optical emission and ionization, J. Geophys. Res., 79, 1459, 1974.

Berger, M. J., S. M. Seltzer and K. Maeda, Energy deposition by auroral electrons in the atmosphere, J. Atmos. Terr. Phys., 32, 1015, 1970.

Berger, M. J., S. M. Seltzer and K. Maeda, Some new results on electron transport in the atmosphere, J. Atmos. Terr. Phys., 36, 591, 1974.

Crutzen, P. J., I. S. A. Isaksen and G. C. Reid, Solar proton events: Stratospheric sources of nitric oxide, Science, 189, 457, 1975.

Gledhill, J. A., Aeronomic effects of the south atlantic anomaly, Rev. Geophys. Space Phys., 14, 173, 1976.

Gledhill, J. A. and R. A. Hoffman, Nighttime observations of 0.2- to 26-keV electrons in the South Atlantic Anomaly made by Atmosphere Explorer C, J. Geophys. Res., 86, 6739, 1981.

Gough, M. P. and H. L. Collin, Energetic electron precipitation as a source of ionization in the nighttime D region over the midlatitude rocket range, South Uist, J. Atmos. Terr. Phys., 35, 835, 1973.

Imhof, W. L., R. R. Anderson, J. B. Reagan and E. E. Gains, The significance of vlf transmitters in the precipitation of inner belt electrons, J. Geophys. Res., 86, 11225, 1981.

Koons, H. C., B. C. Edgar and A. L. Vampola, Precipitation of inner zone electrons by whistler mode waves from the vlf transmitters UMS and NWC, J. Geophys. Res., 86, 640, 1981.

Larsen, T. R., J. B. Reagan, W. L. Imhof, L. E. Montbriand and J. S. Belrose, A coordinated study of energetic electron precipitation and D region electron concentrations over Ottawa during disturbed conditions, J. Geophys. Res., 81, 2200, 1976.

Luhmann, J. G., Auroral electron spectra in the atmosphere, J. Atmos. Terr. Phys., 38, 605, 1976.

Luhmann, J. G., Auroral bremsstrahlung in the atmosphere, J. Atmos. Terr. Phys., 39, 595, 1977.

Lyons, L. R., R. M. Thorne and C. F. Kennel, Pitch angle diffusion of radiation belt electrons within the plasmasphere, J. Geophys. Res., 77, 3455, 1972.

Lyons, L. R. and R. M. Thorne, Equilibrium structure of radiation belt electrons, J. Geophys. Res., 78, 2142, 1973.

Manson, A. H. and M. W. J. Merry, Particle influx and the 'winter anomaly' in the mid-latitude (L = 2.5-3.5) lower ionosphere, J. Atmos. Terr. Phys., 32, 1169, 1970.

Markson, R., Solar modulation of atmospheric electrification and possible implications for the sun-weather relationship, Nature, 273, 103, 1978.

Meira, L. G., Jr., Rocket measurements of upper atmospheric nitric oxide and their consequences to the lower ionosphere, J. Geophys. Res., 76, 202, 1971.

Mohnen, V. A. and C. S. Kiang, Ion-molecule interactions of atmospheric importance, ASRC-SUNY Publ. No. 681, 1978.

Potemra, T. A. and A. J. Zmuda, Precipitating energetic electrons as an ionization source in the mid-latitude nighttime D region, J. Geophys. Res., 75, 7161, 1970.

Potemra, T. A., Precipitating energetic electrons in the mid-latitude lower ionosphere, in Physics and Chemistry of the Upper Atmosphere, edited by B. M. McCormac, p. 67, D. Reidel, Dordrecht, Netherlands, 1973.

Potemra, T. A., Ionizing radiation affecting the lower ionosphere, in ELF-VLF Radio Wave Propagation, edited by J. A. Holtet, p. 21, D. Reidel, Dordrecht, Netherlands, 1974.

Reagan, J. B., Ionization processes, in Dynamical and Chemical Coupling Between the Neutral and Ionized Atmosphere, edited by B. Grandal and J. A. Holtet, p. 145, D. Reidel, Dordrecht, Netherlands, 1977.

Reagan, J. A., R. W. Nightingale, R.E. Meyerott, R. C. Gunton, R. G. Johnson, J. E. Evans and W. L. Imhof, Effects of the August 1972 solar particle events on stratospheric ozone, Tech. Report LMSC-D630455, Lockheed Palo Alto Res. Lab., Palo Alto, Calif., 1978.

Rees, M. H., Auroral ionization and excitation by incident energetic electrons, Planet. Space Sci., 11, 1209, 1963.

Roberts, W. O. and R. H. Olson, Geomagnetic storms and wintertime 300-mb trough development in the northern Pacific-North America area, J. Atmos. Sci., 30, 135, 1973a.

Roberts, W. O. and R. H. Olson, New evidence for effects of variable solar corpuscular emission on the weather, Rev. Geophys. Space Phys., 11, 731, 1973b.

Rosenberg, T. J. and L. J. Lanzerotti, Direct energy inputs to the middle atmosphere, NASA Report on the Workshop on the Role of the Electrodynamics of the Middle Atmosphere on Solar Terrestrial Coupling, edited by Nelson C. Maynard, Reston, Virginia, 1979.

Spjeldvik, W. N. and R. M. Thorne, The cause of storm after effects in the middle latitude D region, J. Atmos. Terr. Phys., 37, 777, 1975.

Spjeldvik, W. N. and R. M. Thorne, Maintenance of the middle-latitude nocturnal D-layer by energetic electron precipitation, J. Pure and Applied Geophys., 114, 497, 1976.

Stamnes, K., On the two-stream approach to electron transport and thermalization, J. Geophys. Res., 86, 2405, 1981.

Strobel, D. F., Nitric oxide in the D region, J. Geophys. Res., 77, 1337, 1972.

Thorne, R. M., Energetic radiation belt electron precipitation: A natural depletion mechanism for stratospheric ozone, Science, 195, 287, 1977.

Torr, D. G., M. R. Torr, R. A. Hoffman and J. C. G. Walker, Global characteristics of 0.2 to 26 keV charged particles at F region altitudes, Geophys. Res. Lett., 3, 305, 1976.

Tulinov, V. F., L. V. Shibraeva and S. G. Jakovlev, Space Research IX, North-Holland, Amsterdam, 1969.

Vampola, A. L., Energetic electrons above the outer zone cutoff, J. Geophys. Res., 74, 1254, 1969.

Vampola, A. L., VLF transmission induced slot electron precipitation, Geophys. Res. Lett., 4, 569, 1977.

Vampola, A. L. and G. A. Kuck, Induced precipitation of inner zone electrons 1. Observations, J. Geophys. Res., 83, 2543, 1978.

Walt, M., W. M. MacDonald and W. E. Francis, Penetration of auroral electrons into the atmosphere, Physics of the Magnetosphere, edited by R. L. Carovillano, D. Reidel, Dordrecht, Netherlands, pp. 534-556, 1969.

LABORATORY OPERATIONS

The Laboratory Operations of The Aerospace Corporation is conducting experimental and theoretical investigations necessary for the evaluation and application of scientific advances to new military space systems. Versatility and flexibility have been developed to a high degree by the laboratory personnel in dealing with the many problems encountered in the nation's rapidly developing space systems. Expertise in the latest scientific developments is vital to the accomplishment of tasks related to these problems. The laboratories that contribute to this research are:

Aerophysics Laboratory: Launch vehicle and reentry aerodynamics and heat transfer, propulsion chemistry and fluid mechanics, structural mechanics, flight dynamics; high-temperature thermomechanics, gas kinetics and radiation; research in environmental chemistry and contamination; cw and pulsed chemical laser development including chemical kinetics, spectroscopy, optical resonators and beam pointing, atmospheric propagation, laser effects and countermeasures.

Chemistry and Physics Laboratory: Atmospheric chemical reactions, atmospheric optics, light scattering, state-specific chemical reactions and radiation transport in rocket plumes, applied laser spectroscopy, laser chemistry, battery electrochemistry, space vacuum and radiation effects on materials, lubrication and surface phenomena, thermionic emission, photosensitive materials and detectors, atomic frequency standards, and bioenvironmental research and monitoring.

Electronics Research Laboratory: Microelectronics, GaAs low-noise and power devices, semiconductor lasers, electromagnetic and optical propagation phenomena, quantum electronics, laser communications, lidar, and electro-optics, communication sciences, applied electronics, semiconductor crystal and device physics, radiometric imaging, millimeter-wave and microwave technology.

Information Sciences Research Office: Program verification, program translation, performance-sensitive system design, distributed architectures for spaceborne computers, fault-tolerant computer systems, artificial intelligence, and microelectronics applications.

Materials Sciences Laboratory: Development of new materials: metal matrix composites, polymers, and new forms of carbon; component failure analysis and reliability; fracture mechanics and stress corrosion; evaluation of materials in space environment; materials performance in space transportation systems; analysis of systems vulnerability and survivability in enemy-induced environments.

Space Sciences Laboratory: Atmospheric and ionospheric physics, radiation from the atmosphere, density and composition of the upper atmosphere, auroras and airglow, magnetospheric physics, cosmic rays, generation and propagation of plasma waves in the magnetosphere, solar physics, infrared astronomy; the effects of nuclear explosions, magnetic storms, and solar activity on the earth's atmosphere, ionosphere, and magnetosphere; the effects of optical, electromagnetic, and particulate radiations in space on space systems.

. . .


DAT
ILM